



Minimal cooling speed for glass transition in a simple solvable energy landscape model



J. Quetzalcóatl Toledo-Marín^a, Isaac Pérez Castillo^b, Gerardo G. Naumis^{a,c,*}

^a Departamento de Física-Química, Instituto de Física, Universidad Nacional Autónoma de México (UNAM), Apartado Postal 20-364, 01000 México, Distrito Federal, Mexico

^b Departamento de Sistemas Complejos, Instituto de Física, Universidad Nacional Autónoma de México (UNAM), Apartado Postal 20-364, 01000 México, Distrito Federal, Mexico

^c School of Physics Astronomy and Computational Sciences, George Mason University, Fairfax, VA 22030, USA

HIGHLIGHTS

- A simple solvable energy model landscape is presented.
- This model captures a glass transition or crystallization.
- The minimal cooling rate to obtain a glass is related to the thermal history.
- The glass transition temperature has a logarithmic dependence on cooling rate.

ARTICLE INFO

Article history:

Received 11 October 2015

Received in revised form 19 November 2015

Available online 2 February 2016

Keywords:

Glass transition

Phase transitions

Non-equilibrium systems

ABSTRACT

The minimal cooling speed required to form a glass is obtained for a simple solvable energy landscape model. The model, made from a two-level system modified to include the topology of the energy landscape, is able to capture either a glass transition or a crystallization depending on the cooling rate. In this setup, the minimal cooling speed to achieve glass formation is then found to be related with the crystallization relaxation time, energy barrier and with the thermal history. In particular, we obtain that the thermal history encodes small fluctuations around the equilibrium population which are exponentially amplified near the glass transition, which mathematically corresponds to the boundary layer of the master equation. The change in the glass transition temperature is also found as a function of the cooling rate. Finally, to verify our analytical results, a kinetic Monte Carlo simulation was implemented.

© 2016 Elsevier B.V. All rights reserved.

1. Introduction

The importance of glassy materials in our societies is indisputable. It is an essential component of numerous products that we use on daily basis, most often without noticing it. Even though the glass formation process has been extensively studied using different approaches, it remains an open and puzzling problem, and this far our best understanding of the process is barely limited at the phenomenological level [1–12]. The reason behind this situation is that glass formation is mainly a non-equilibrium process [13].

* Corresponding author at: Departamento de Física-Química, Instituto de Física, Universidad Nacional Autónoma de México (UNAM), Apartado Postal 20-364, 01000 México, Distrito Federal, Mexico.

E-mail address: naumis@fisica.unam.mx (G.G. Naumis).

From a fundamental and technological point of view, the most important variable for glass formation is the cooling speed [10,14]. Indeed, the industrial use of metallic glasses has been hampered for a while due to the high cooling speed required in order to form glasses [15–17]. However, by chemical modification, the cooling process of metallic glasses has been improved a lot [18], and very recently it was possible to form a monocomponent metallic glass, achieved by hyperquenching [19]. Regarding the relationship between chemical composition and minimal cooling speed, Phillips [20] observed that for several chalcogenides, this minimal speed is a function of the rigidity. His initial observation was the starting point for an extensive investigation on the rigidity of glasses, yet this observation has not been quantitatively obtained in glass models although it is related with the energy landscape topology when the rigidity is taken into account [21–24].

As the cooling rate effects on glass formation are poorly understood, one would expect that in any sensible model of glass transition, the phase transition to the crystal should be included for low cooling rates. However, this point has been overlooked in several theories of glass formation, even though phase change materials have a paramount importance for information storage technologies. For example, recently it has been possible to access the full temperature range of the crystallization process, including the full supercooled liquid regime, for the chalcogenide-based materials used to store information in rewritable DVDs [25]. On the other hand, the energy landscape has been a useful picture to understand glass transition [9] but, due to its complicate high dimensional topology, it is difficult to understand how cooling rates are related with the topological sampling.

Simple models of glass transition have been introduced trying to capture the physical properties of this phenomenon (see for instance [26,27]). In particular, in a previous paper, a minimal simple solvable model of landscape that can display either a crystalline phase or a glass transition depending on the cooling rate was presented by one of us [28]. Such model, a refinement of a two-level system (TLS) model previously studied [29–33], included the most basic ingredients for a glass formation process: metastable states and the landscape topology [28]. As a result, the model was able to produce either a true phase transition or a glass transition in the thermodynamic limit [28]. Nonetheless, there were important questions that were not tackled in our previous publication. In particular, it was not clear how to define a critical cooling speed that separates the transition either to a glass or to a crystal, and how this critical speed depends upon the physical characteristics of the system like relaxation times, energy barriers and the thermal history. In this study, we answer these open questions by obtaining analytical expressions to all these quantities. To verify these analytic calculations, a kinetic Monte Carlo is performed showing an excellent agreement.

This article is organized as follows: Section 2 is devoted to recall the model and its features, as well as to obtain the system's behavior and an analytical expression of the glassy state when a given cooling protocol is applied [28]. In Section 3, we derive the characteristic relaxation time of our system. In Section 4 we obtain the relation between the metastable state, the cooling rate, the characteristic relaxation time and the thermal history of our system; here we also obtain the expression which relates the glass transition temperature with the energy barrier and the cooling rate. In Section 5 we compare our results with kinetic Monte Carlo simulation. Finally, in Section 6 we summarize and discuss our findings.

2. Revisiting a solvable energy landscape model: glass transition and crystallization

The model is defined as follows: topologically there are many basins in the energy landscape, each corresponding to a possible state of the system [28]. However, there are only two energetic levels (see Fig. 1). One of these levels has energy $E_0 = 0$, while the other has energy $E_1 = N\epsilon_1$, where N corresponds to the number of particles in the system and ϵ_1 gives the energy scale. Within the model, the crystalline state is the one with zero energy, while there are g_1 glassy states with energy E_1 . It turns out that $g_1 = \exp(N \ln \Omega)$, where Ω is just the complexity of the energy-landscape [9], taken as $\Omega = 2$ for simplicity. Finally, the model assumes that the energy barriers that separates each of the g_1 states among them are the same, while the barriers that separate each of the glassy states from the crystal are also equal and given by V (see Fig. 1).

When the system is in equilibrium at a certain temperature T , the canonical partition function¹ reads:

$$Z(T, N) = 1 + g_1 e^{-E_1/T}, \quad (1)$$

and the equilibrium probability $p_0(T)$ of the system having energy E_1 is given by the usual ensemble average:

$$p_0(T) = \frac{g_1 e^{-E_1/T}}{1 + g_1 e^{-E_1/T}}. \quad (2)$$

As shown in Ref. [28], for this equilibrium population the system experiences a phase transition associated with crystallization when the temperature crosses the critical value $T_c = \epsilon_1 / \log(2)$.

To study the system out of equilibrium, one observes that due to the simple landscape topology, all transition probabilities per time between metastable states are the same. The transition probability per time from each metastable state to the ground state is also equal for all metastable states [28]. In this setup, the probability $p(t)$ of finding the system with energy E_1 at time t obeys the following master equation:

$$\dot{p}(t) = -\Gamma_{10} p(t) + \Gamma_{01} g_1 (1 - p(t)), \quad (3)$$

¹ From now on Boltzmann's constant $k_B = 1$.

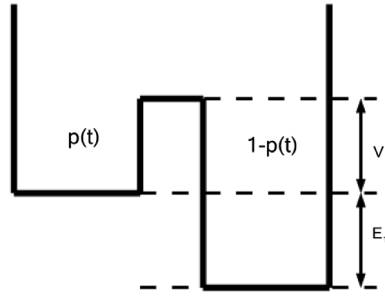


Fig. 1. The two level system energy landscape, showing the barrier height V and the asymmetry E_1 between the two levels. The population of the upper well is $p(t)$ [28].

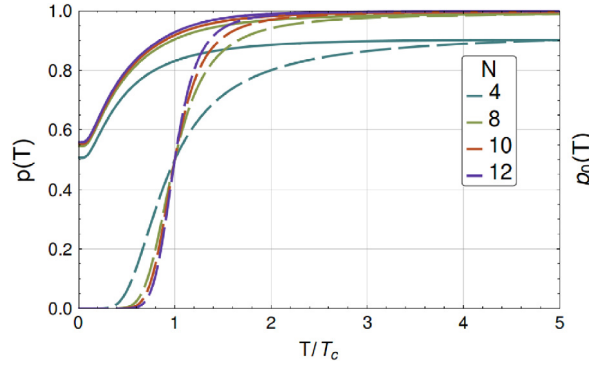


Fig. 2. $p(T)$ in equilibrium (dashed lines) and non-equilibrium (solid lines) with a hyperbolic cooling protocol. The parameters were fixed at $T_0 = 5T_c$, $V = 0.5$, $R = 20$ and $\Gamma_0 = 1$.

where Γ_{10} corresponds to the transition probability per time of going from a state with energy E_1 to the ground state 0 and Γ_{01} for the reverse transition. The detailed balance condition yields:

$$\frac{\Gamma_{01}}{\Gamma_{10}} = e^{-E_1/T} \tag{4}$$

and $\Gamma_{10} = \Gamma_0 e^{-V/T}$, where V is the height of the barrier wall between state 1 and state 0, and Γ_0 is a small frequency of oscillation at the bottom of the wells which sets the timescale.

Now we are interested in the process of arresting the system in one of the higher energy states by a rapid cooling, as it happens with glasses. In particular, we are interested in studying the system as the temperature goes from $T > T_c$ to $T = 0$ by a cooling rate determined by a given protocol $T(t)$. Notice that since $T = T(t)$, the population described by Eq. (3) will be denoted at times by $p(T)$, not to be confused with the equilibrium probability $p_0(T)$. Experimentally, a linear cooling is usually used. However, for the purposes of the model, it is much simpler to use a hyperbolic cooling protocol $T(t) = T_0/(1 + Rt)$, where T_0 is the initial temperature at which the system is in equilibrium and R is the cooling rate. The results using both protocols are similar since basically the equations can be approximated using the boundary layer theory of differential equations [32,28]. By boundary layer, we mean that in Eq. (3), the time derivative can be neglected above T_c and the system behaves as an equilibrated system. However, as $T \rightarrow T_c$, the derivative cannot be longer neglected, since its order is similar to the other terms. A similar situation happens with the Navier–Stokes equations in fluids, which are reduced to Euler equations far from the boundary, but near the boundary the full equation is needed, producing effects like turbulence.

The solution to the master equation (3) given the cooling protocol is:

$$P(x, \delta) = e^{\frac{1}{\delta} \left(x + g_1 \frac{x^{\mu+1}}{\mu+1} \right)} \left(P(0, \delta) - \frac{g_1}{\delta} \int_0^x dy y^\mu e^{-\frac{1}{\delta} \left(y + g_1 \frac{y^{\mu+1}}{\mu+1} \right)} \right), \tag{5}$$

where $p(t) = P(x(t), \delta)$ with $x(t) = \exp(-V/T(t))$, $\delta = RV/\Gamma_0 T_0$ is the dimensionless cooling rate, and the parameter $\mu = E_1/V$ measures the asymmetry of the well.

According to Eqs. (2) and (5), and as we can appreciate in Fig. 2 for different number of particles N , when the system is cooled down to $T = 0$ there is a residual population, i.e., $p(T = 0) \neq 0$ ($P(x = 0, \delta) \neq 0$) indicative of a glassy behavior due to the trapping of the system in a metastable state [31,28]. In fact, we can obtain an analytical expression for $P(x = 0, \delta)$ as

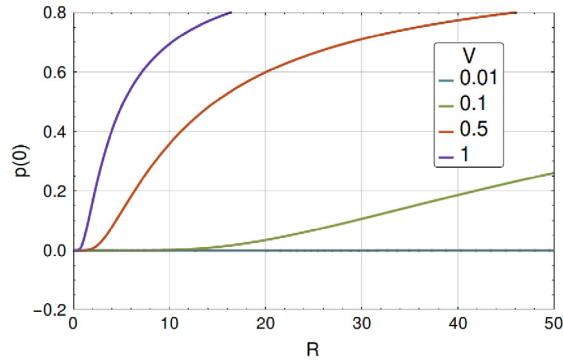


Fig. 3. $p(T = 0)$ for different barrier heights. The parameters were fixed at $T_0 = 5T_c$, $N = 500$ and $\Gamma_0 = 1$.

follows: From Eq. (5), we may write $P(0, \delta)$ as a function of the rest of the terms, i.e.

$$P(0, \delta) = P(x, \delta) e^{-\frac{1}{\delta} \left(x + g_1 \frac{x^{\mu+1}}{\mu+1} \right)} + \frac{g_1}{\delta} \int_0^x dy y^\mu e^{-\frac{1}{\delta} \left(y + g_1 \frac{y^{\mu+1}}{\mu+1} \right)}. \quad (6)$$

Now, notice that in the context of the process in which we are interested, $P(0, \delta)$ is the final configuration of the system while $P(x, \delta)$ is the initial condition. Let us assume that the initial condition is such that the system is in thermal equilibrium at $T_0 > T_c$ before being cooled, and we denote $x_0 = e^{-V/T_0}$. Thus we use Eq. (2) to express $P(x_0, \delta)$ and we obtain the following expression:

$$P(0, \delta) = \frac{g_1 x_0^\mu}{1 + g_1 x_0^\mu} e^{-\frac{1}{\delta} \left(x_0 + g_1 \frac{x_0^{\mu+1}}{\mu+1} \right)} + \frac{g_1}{\delta} \int_0^{x_0} dy y^\mu e^{-\frac{1}{\delta} \left(y + g_1 \frac{y^{\mu+1}}{\mu+1} \right)}. \quad (7)$$

As we can see in Fig. 3, the residual population given by Eq. (7) has a strong dependence of the barrier height and the cooling rate. We will come back to this point on Section 4.

3. Characteristic relaxation times of the model

Let us now focus on quantifying the dependence of this residual population on the energy landscape. In particular we would like to have a criterion to discern *how fast one should cool the system down to obtain a residual population*.

Clearly, in order to trap the system the cooling must be such that the system does not have enough time to reach equilibrium, so let us first determine the characteristic relaxation time of the system. To do so, we take the parameters of the model to be fixed but the system is not in equilibrium, i.e., the temperature is fixed and the system is perturbed in such a way that at $t = 0$, the population is $p(t = 0) = \rho$, where ρ takes values between 0 and 1. Looking from the master equation (3) and the detailed balance condition (4) how the system relaxes towards $p_0(T)$, we obtain an exponential decay:

$$p(t) = p_0(T) + (\rho - p_0(T)) \exp(-t/\tau(T)), \quad (8)$$

from which we define the characteristic relaxation time $\tau(T) = 1/(\Gamma_{10} + \Gamma_{01}g_1)$.

Notice that for $N \gg 1$ the characteristic relaxation time (8) goes as $\sim (g_1\Gamma_{01})^{-1}$ for $T > T_c$, while for $T < T_c$ goes as $\sim (\Gamma_{10})^{-1}$ (see Fig. 4). In particular, when T crosses the critical temperature T_c , $\tau(T)$ has a jump of height (see Fig. 4),

$$\Delta\tau(T_c) \approx \Gamma_{10}^{-1} - (g_1\Gamma_{01})^{-1}. \quad (9)$$

However, since the relaxation time for $T < T_c$ is much bigger than the corresponding time for $T > T_c$, we can identify the jump with the relaxation time at T_c taken by approaching the discontinuity from the left, i.e., from $T < T_c$. Thus $\tau_L(T_c) \approx \Delta\tau(T_c)$ from where it follows,

$$\tau_L(T_c) \approx \Gamma_0^{-1} \exp(V/T_c). \quad (10)$$

Hence, when $T > T_c$ and the system has energy 0, the transition time is virtually zero, whereas when $T < T_c$ and the system has energy E_1 , the transition time grows exponentially with V/T .

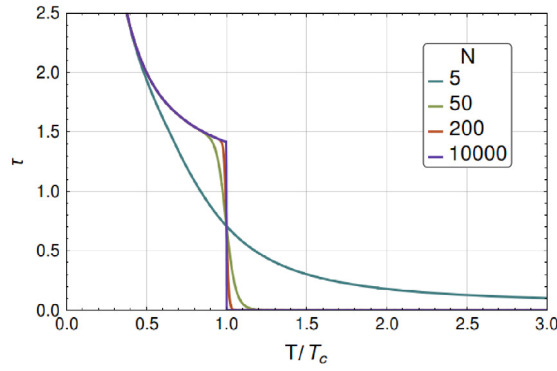


Fig. 4. Characteristic relaxation time $\tau(T)$ as a function of the number of particles N , with fixed parameters $V = 0.5$, $\epsilon_1 = 1$, $\Gamma_0 = 1$. Notice the jump $\Delta\tau$ of the relaxation time at T_c .

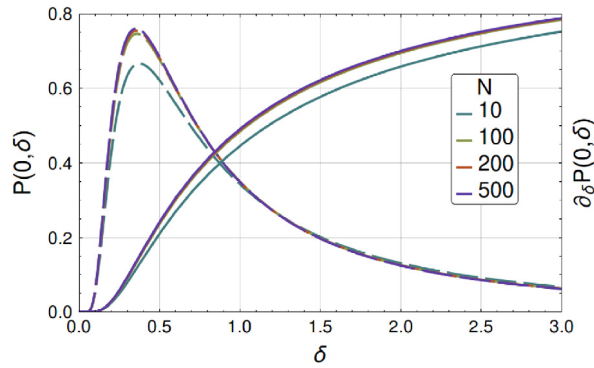


Fig. 5. Here we plot $P(0, \delta)$ (continuous lines) and $\frac{\partial P(0, \delta)}{\partial \delta}$ (dashed lines) as a function of δ for different number of particles N . We fixed the parameters at $T_0 = 5T_c$, $\Gamma_0 = 1$, $V = 0.5$, $\epsilon_1 = 1$.

4. Critical cooling rate and glass transition

As we have seen above, for a certain cooling rate R there is a non-zero probability of finding the system in state 1 at $T = 0$, and the time needed for the system to transition from state 1 to state 0 goes as $\exp(V/T)$ when $T < T_c$. We would like now to have simple criterion that relates the cooling rate and a substantial residual population indicative of a glassy behavior. Noticing that Eq. (7) is continuous and reaches zero only when $\delta = 0$, we then take as a criterion the inflection point of $p(0, \delta)$ (as shown in Fig. 5). Thus by denoting δ_c the cooling rate at the inflection point, we can associate a strong glass forming tendency (SGFT) for $\delta > \delta_c$.

To find the dependence of δ_c as a function of the parameters of the model we proceed as follows. We write Eq. (7) as $P(0; \delta, \mu, N) = I_1 + I_2$, where:

$$I_1 = \frac{g_1 x_0^\mu}{1 + g_1 x_0^\mu} \exp \left[-\frac{1}{\delta} \left(x_0 + g_1 \frac{x_0^{\mu+1}}{\mu + 1} \right) \right], \tag{11}$$

$$I_2 = \frac{g_1}{\delta} \int_0^{x_0} dy y^\mu \exp \left[-\frac{1}{\delta} \left(y + g_1 \frac{y^{\mu+1}}{\mu + 1} \right) \right].$$

Integrating the expression of I_2 in Eq. (11) by parts leads to

$$I_2 = 1 - e^{-\frac{1}{\delta} \left(x_0 + g_1 \frac{x_0^{\mu+1}}{\mu+1} \right)} - \int_0^{x_0} \frac{dy}{\delta} e^{-\frac{y}{\delta} \left(1 + g_1 \frac{y^\mu}{\mu+1} \right)}. \tag{12}$$

Let us denote $x_c = x(T_c)$. In the thermodynamic limit where $N \gg 1$, for $y < x_c$ we have that $g_1 \frac{y^\mu}{\mu+1} \simeq 0$, whereas if $y > x_c$ results in $g_1 \frac{y^\mu}{\mu+1} \gg 1$. Thus, we may approximate the last term in expression (12) as:

$$- \int_0^{x_0} \frac{dy}{\delta} e^{-\frac{y}{\delta} \left(1 + g_1 \frac{y^\mu}{\mu+1} \right)} \simeq e^{-y/\delta} \Big|_0^{x_c}. \tag{13}$$

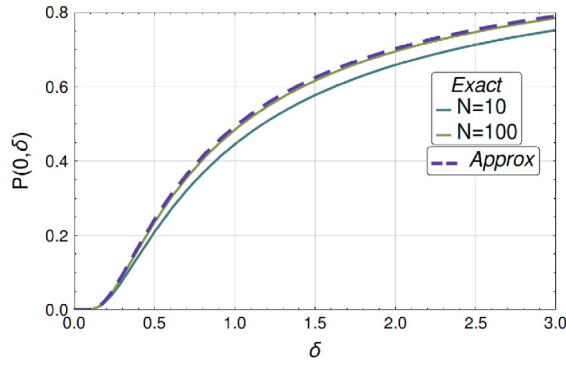


Fig. 6. Comparison between Eqs. (15) and (7) as a function of δ . The parameters were fixed at $V = 0.5$, $\epsilon_1 = 1$, $T_0 = 5T_c$, $\Gamma_0 = 1$.

Thus, substituting Eqs. (12) and (13) in Eq. (7) yields:

$$P(0, \delta) \simeq -\frac{1}{1+g_1 x_0^\mu} e^{-\frac{1}{\delta} \left(x_0 + g_1 \frac{x_0^{\mu+1}}{\mu+1} \right)} + \exp\left(-\frac{x_c}{\delta}\right). \quad (14)$$

Since $x_0 > x_c$, then Eq. (14) can be approximated as:

$$P(0, \delta) \simeq \exp\left(-\frac{x_c}{\delta}\right). \quad (15)$$

Finally, writing Eq. (15) in terms of R yields:

$$p(T=0) \approx \exp\left(-\frac{T_0 \Gamma_{10}^c}{RV}\right), \quad (16)$$

where

$$\Gamma_{10}^c = \Gamma_0 e^{-V/T_c}. \quad (17)$$

We may also approximate equation (5) in the thermodynamic limit and obtain

$$P(x, \delta) = \begin{cases} 1, & x \geq x_c \\ \exp\left(-\frac{1}{\delta}(x_c - x)\right), & x \leq x_c. \end{cases} \quad (18)$$

In Fig. 6 we have compared the exact result and the approximation of $P(0, \delta)$ (Eqs. (7) and (15)). We can clearly appreciate how the exact results become close to our approximation Eq. (16) as N increases. Notice that expression (16) relates the residual population with the cooling rate R and the characteristic time τ in a very simple and intuitive manner. This result tells us that trapping the system in the metastable state ultimately depends on the cooling rate solely applied in a region close to the phase transition zone [34], although there is a catch.

Suppose that we cool the system starting from T_1 with a cooling rate R_1 , and we repeat the process starting from $T_2 \neq T_1$ with a cooling rate $R_2 \neq R_1$. The residual population $p(0)$ may be the same in both cases provided $T_1/R_1 = T_2/R_2$. This implies that if $T_1 > T_2$ then $R_1 > R_2$, i.e., to trap the system in state 1 starting from T_1 we would need a cooling rate R_1 bigger than the one needed if the cooling started at $T_2 < T_1$. Thus, we would be compelled to assume that the “best” way to trap the system in our model would be to set the initial temperature T_0 as close as possible to T_c . However, in our model T_0 is the initial temperature in which the system is in thermodynamical equilibrium. Fig. 2 illustrates this idea, i.e., even though the transition occurs in T_c the non-equilibrium system’s path differs from the equilibrium system’s path even before reaching T_c , therefore there is a lower bound for T_0 . This means that the thermal history encodes small fluctuations around the equilibrium population which are exponentially amplified near the glass transition. This region of the glass transition corresponds precisely to the boundary layer limit.

Finally, we can get the critical dimensionless cooling rate for obtaining glasses by calculating the inflection point of the approximation given by Eq. (15). As a result, the inflection point of $P(0, \delta)$ as a function of δ is given by,

$$\delta_G = x_c/2. \quad (19)$$

Evaluating δ_G in our approximation (Eq. (15)) gives always the same population at the inflection point $P(0, \delta_G) = e^{-2} \approx 0.13$. This means that below δ_G there is a probability of a residual population lower than ~ 0.13 .

Now, in terms of the T -parameters, Eq. (19) yields the critical cooling rate R_G :

$$R_G = e^{-V/T_c} \frac{\Gamma_0 T_0}{2V} \quad (20)$$

which is the minimal R required to get a glass.

Notice that from Eq. (20), when V is small ($V \simeq 0$), the cooling rate for a SGFT goes as $\sim V^{-1}$, that is, the critical cooling rate grows as the barrier height diminishes. When the barrier height is large, the necessary cooling rate is small for a SGFT, as can be seen in Fig. 3.

To interpret such result, let us write R_G in terms of the characteristic relaxation time to crystallization at T_c , given by Eq. (10), the initial temperature in equilibrium T_0 and the barrier height, i.e.,

$$R_G = \frac{T_0}{2V\tau_L(T_c)}. \tag{21}$$

The previous result confirms the intuitive perception of the glass transition, i.e., that the cooling rate must be faster than the crystallization time, while the barrier height also plays a role. In other words, the system gets stuck in a glassy state due to a lack of time for exploring the landscape. However, Eq. (21) indicates the importance of the initial conditions through T_0 . Within this model, the absence of a crystal is indicative of an infinite crystallization time as happens in some systems which never crystallize unless pressure is applied.

The model also provides a relationship between the glass transition temperature T_g and the cooling rate. Experimentally, T_g is obtained from a peak in the specific heat. In our model, the heat capacity per particle is given by $\epsilon_1 \frac{\partial p(T)}{\partial T}$. Thus, the glass transition temperature T_g occurs when the specific heat capacity derivative is a maximum, i.e.,

$$\left\{ \epsilon_1 \frac{\partial^3 p(T)}{\partial^3 T} \right\}_{T_g} = 0. \tag{22}$$

This leads to the following transcendental equation that relates T_g with the parameters of the model,

$$\frac{T_0^2 V}{R^2 T_g^6} \left(\frac{1}{\tau(T_g)} \right)^2 + \frac{3T_0}{RT_g^2} \left(\frac{-2V}{T_g^3} + \frac{V^2}{T_g^4} \right) \frac{1}{\tau(T_g)} - \frac{6V}{T_g^4} - \frac{6V^2}{T_g^5} + \frac{V^3}{T_g^6} = 0, \tag{23}$$

where $\tau(T_g)$ is the characteristic relaxation time at the glass transition temperature, i.e., $\tau(T_g) = \Gamma_0^{-1} e^{V/T_g}$. This relaxation time at T_g is exactly the same as the one obtained in Ref. [35] using different kind of arguments.

It is worth mentioning that this equation indicates that in general T_g depends on the cooling rate R , as observed experimentally and in other models of glass formation [35]. In forthcoming papers, we will explore the rich behavior in the parameter space of Eq. (23). Yet, it is possible to get the experimentally observed logarithm change with the cooling rate of T_g by adapting the approach used by Trachenko and Brazhkin [35]. To do so, it is important to observe that our cooling protocol is not linear, as in the case studied by Trachenko et al. [35]. Here the characteristic relaxation time at T_g is given by,

$$\tau(T_g) = \frac{T_0}{R} (T_2^{-1} - T_1^{-1}) \tag{24}$$

where T_2 and T_1 are the two temperatures which define the temperature range of the transformation (with $T_1 > T_2$). This result can be combined with $\tau(T_g) = \Gamma_0^{-1} e^{V/T_g}$ to get,

$$T_g = \frac{V}{\ln\left(\frac{\Delta T}{T_0}\right) - \ln(\Gamma_0^{-1} R)} \tag{25}$$

where $\overline{\Delta T}$ is defined as a reduced temperature range,

$$\overline{\Delta T} = \frac{T_0^2}{T_2 T_1} (T_1 - T_2). \tag{26}$$

Eq. (25) predicts a logarithm change of T_g with the cooling rate, as observed experimentally, and coincides with the expression obtained by Trachenko et al. [35].

5. Kinetic Monte Carlo simulation

To assess the validity of our mathematical analysis we have compared our analytic results with a Kinetic Monte Carlo (KMC) simulation. The simulation was done in a standard way (see for instance [34]). The (residence) time Δt_{ij} the system spends in state i ($i, j = \{0, 1\}$, $i \neq j$), given the frozen state condition is not fulfilled [34], is determined by the relation:

$$-\log(x) = \int_t^{t+\Delta t_{ij}} dt' W_{ij}(t'), \tag{27}$$

with

$$\begin{aligned} W_{10}(t) &= \Gamma_{10}(t), \\ W_{01}(t) &= g_1 \Gamma_{01}(t), \end{aligned} \tag{28}$$

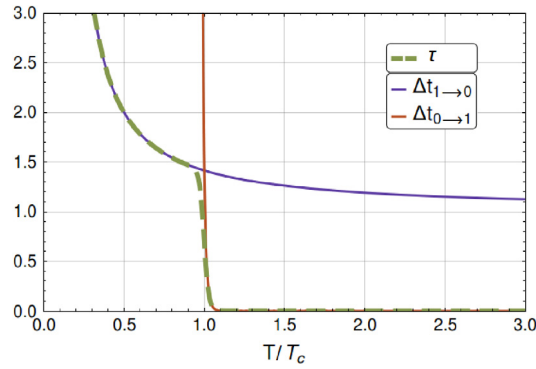


Fig. 7. KMC transition times (Eqs. (29) and (30)) for a cooling rate $R = 0.01$ (continuous lines) and characteristic relaxation time τ obtained from Eq. (8) (dashed line). We have fixed the parameters to $T_0 = 5T_c$, $V = 0.5$, $\epsilon_1 = 1$, $N = 100$.

and x a uniformly distributed random number between 0 and 1. Thus, from relation (27) and expressions (28) we obtain:

$$\Delta t_{10} = -\frac{T_0}{VR} \log \left(1 + \frac{\log(x)VR}{\Gamma_0 T_0} e^{V(1+Rt)/T_0} \right), \quad (29)$$

$$\Delta t_{01} = -\frac{T_0}{(V + E_1)R} \log \left(1 + \frac{\log(x)(V + E_1)R}{\Gamma_0 T_0} \exp(-N \log(2) + (V + E_1)(1 + Rt)/T_0) \right). \quad (30)$$

In Fig. 7 we have plotted expressions (29) and (30) for $x = e^{-1}$ and a small cooling rate R , i.e., a quasi-equilibrium cooling rate, and we have compared it with the characteristic relaxation time τ as a function of T . Notice that when $T > T_c$, $\Delta t_{10} > \Delta t_{01}$, whereas when $T < T_c$ results in $\Delta t_{10} < \Delta t_{01}$. Furthermore, when $T > T_c$ the residence time Δt_{01} corresponds to the system's characteristic relaxation time, while when $T < T_c$ the residence time Δt_{10} correspond to the system's characteristic relaxation time.

In Fig. 8 we have compared $p(T)$, the exact form (Eq. (5) as a function of $T(t)$ (left) and the approximation form (Eq. (18)) (right), with our KMC simulation for different cooling rates. As for Fig. 9, we have compared the approximation to the residual population (Eq. (15)) with our KMC simulation. The match between our exact results and the KMC simulation, and also our approximations and the KMC simulation is outstanding. We should stress the fact that the computational cost by the KMC simulation is much less than the numerical evaluation of $p(T)$ for large N .

Following [34], given that the system is initially in state i , the probability that it will remain frozen in this state forever is $\exp(-s_i^{(\infty)})$ with:

$$s_i^{(\infty)} \equiv \lim_{t \rightarrow \infty} \int_0^t dt' W_{ij}(t'). \quad (31)$$

In our model this implies that

$$\exp(-s_1^{(\infty)}) = \exp\left(-\frac{x_0}{\delta}\right), \quad (32)$$

$$\exp(-s_0^{(\infty)}) = \exp\left(-\frac{g_1 x_0^{\mu+1}}{\delta(\mu+1)}\right). \quad (33)$$

Notice that at $T_0 = T_c$, the expression (32) is the same as our approximation of $P(0; \delta)$ given by Eq. (15). Therefore, trapping the system in state 1 ultimately depends on doing so at the transition point, although the system's path towards that transition point is relevant. Hence, the system has thermal history.

6. Conclusions

Using a simple energy landscape model that shows a phase transition and a glass transition depending on the cooling rate, we found a relation between the residual population, the characteristic relaxation times, the cooling rate and the thermal history. In particular, the residual population, which is a measure of the glass forming tendency, turns out to have an inflection point as a function of the cooling rate. This allows to define a critical cooling rate in the sense that higher cooling speeds than the critical one results in an increased glass forming tendency. The critical rate depends upon the relaxation time for crystallization, the phase transition temperature and the thermal history. Interestingly, the thermal history produces small fluctuations around the equilibrium population which are exponentially amplified near the glass transition, which

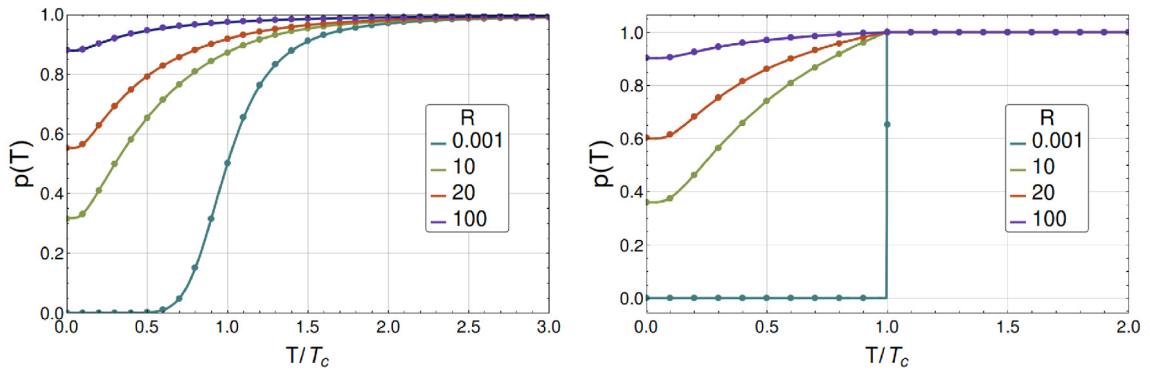


Fig. 8. $p(T)$. Left: Comparison between our exact solution (Eq. (5)) (continuous line) and our KMC simulation (points), for different cooling rates R and number of particles $N = 10$. Right: Comparison between our approximation of $p(T)$ (Eq. (18)) (continuous line) and our KMC simulation (points), for different cooling rates R and number of particles $N = 10^4$. The KMC simulation was done with an ensemble of 10^5 systems. The rest of the parameters were fixed at $T_0 = 5T_c$, $V = 0.5$, $\Gamma_0 = 1$.

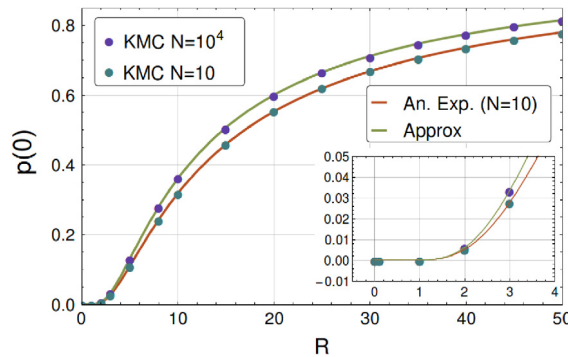


Fig. 9. $p(0)$. Comparison between our exact and approximate expressions (continuous line) and our KMC simulation (points) for different cooling rates R and the following choice of parameters: $N = 10$, $T_0 = 5T_c$, $V = 0.5$, $\Gamma_0 = 1$. The KMC simulation was done with an ensemble of 10^5 systems and $N = \{10, 10^4\}$.

in fact corresponds to the region of the master equation boundary layer. In other words, the thermal history encodes the sensibility to the initial conditions of the system, as happens with turbulence inside the boundary layer.

We have also obtained a widely observed logarithmic increase of the glass transition temperature with the cooling rate also obtained in Ref. [35] by a different approach.

Finally, a kinetic Monte Carlo simulation was performed to check the analytically obtained residual populations and the relaxation times. An excellent agreement was found between both methods. In fact, the relaxation time is a nice interpolation of the residence times obtained from the Monte Carlo. All these results could be used for more realistic energy landscapes, by using connectivity maps [36–38].

Acknowledgments

The authors would like to thank the referees. Special thanks are due to referee 2 for his insightful comments and inquiries.

References

- [1] G.G. Naumis, R. Kerner, Stochastic matrix description of glass transition in ternary chalcogenide systems, *J. Non-Cryst. Solids* 231 (1) (1998) 111–119.
- [2] J. Phillips, Stretched exponential relaxation in molecular and electronic glasses, *Rep. Progr. Phys.* 59 (9) (1996) 1133.
- [3] R. Kerner, G.G. Naumis, Stochastic matrix description of the glass transition, *J. Phys.: Condens. Matter* 12 (8) (2000) 1641.
- [4] M. Micoulaut, G. Naumis, Glass transition temperature variation, cross-linking and structure in network glasses: a stochastic approach, *Europhys. Lett.* 47 (5) (1999) 568.
- [5] P.E. Ramírez-González, L. López-Flores, H. Acuña-Campa, M. Medina-Noyola, Density-temperature-softness scaling of the dynamics of glass-forming soft-sphere liquids, *Phys. Rev. Lett.* 107 (15) (2011) 155701.
- [6] P.G. Debenedetti, *Metastable Liquids: Concepts and Principles*, Princeton University Press, 1996.
- [7] P.G. Debenedetti, F.H. Stillinger, Supercooled liquids and the glass transition, *Nature* 410 (6825) (2001) 259–267.
- [8] F.H. Stillinger, Supercooled liquids, glass transitions, and the kauzmann paradox, *J. Chem. Phys.* 88 (12) (1988) 7818–7825.
- [9] F.H. Stillinger, P.G. Debenedetti, Energy landscape diversity and supercooled liquid properties, *J. Chem. Phys.* 116 (8) (2002) 3353–3361.
- [10] M.M. Smedskjaer, J.C. Mauro, Y. Yue, Prediction of glass hardness using temperature-dependent constraint theory, *Phys. Rev. Lett.* 105 (11) (2010) 115503.
- [11] K. Trachenko, A stress relaxation approach to glass transition, *J. Phys.: Condens. Matter* 18 (19) (2006) L251.

- [12] K. Trachenko, C. Roland, R. Casalini, Relationship between the nonexponentiality of relaxation and relaxation time in the problem of glass transition, *J. Phys. Chem. B* 112 (16) (2008) 5111–5115.
- [13] G.G. Naumis, Variation of the glass transition temperature with rigidity and chemical composition, *Phys. Rev. B* 73 (17) (2006) 172202.
- [14] J.C. Mauro, D.C. Allan, M. Potuzak, Nonequilibrium viscosity of glass, *Phys. Rev. B* 80 (9) (2009) 094204.
- [15] A. Inoue, Stabilization of metallic supercooled liquid and bulk amorphous alloys, *Acta Mater.* 48 (1) (2000) 279–306.
- [16] J. Reyes-Retana, G. Naumis, The effects of si substitution on the glass forming ability of ni–pd–p system, a dft study on crystalline related clusters, *J. Non-Cryst. Solids* 387 (2014) 117–123.
- [17] J. Reyes-Retana, G. Naumis, Ab initio study of si doping effects in pd–ni–p bulk metallic glass, *J. Non-Cryst. Solids* 409 (2015) 49–53.
- [18] M. Ashby, A. Greer, Metallic glasses as structural materials, *Scr. Mater.* 54 (3) (2006) 321–326.
- [19] L. Zhong, J. Wang, H. Sheng, Z. Zhang, S.X. Mao, Formation of monatomic metallic glasses through ultrafast liquid quenching, *Nature* 512 (7513) (2014) 177–180.
- [20] J.C. Phillips, Topology of covalent non-crystalline solids i: Short-range order in chalcogenide alloys, *J. Non-Cryst. Solids* 34 (2) (1979) 153–181.
- [21] G. Naumis, J. Phillips, Bifurcation of stretched exponential relaxation in microscopically homogeneous glasses, *J. Non-Cryst. Solids* 358 (5) (2012) 893–897.
- [22] A. Huerta, G. Naumis, Relationship between glass transition and rigidity in a binary associative fluid, *Phys. Lett. A* 299 (5) (2002) 660–665.
- [23] H.M. Flores-Ruiz, G.G. Naumis, J. Phillips, Heating through the glass transition: A rigidity approach to the boson peak, *Phys. Rev. B* 82 (21) (2010) 214201.
- [24] G. Naumis, G. Cocho, The tails of rank-size distributions due to multiplicative processes: from power laws to stretched exponentials and beta-like functions, *New J. Phys.* 9 (8) (2007) 286.
- [25] P. Zalden, A. von Hoegen, P. Landreman, M. Wuttig, A.M. Lindenberg, How supercooled liquid phase-change materials crystallize: Snapshots after femtosecond optical excitation, *Chem. Mater.* 27 (16) (2015) 5641–5646.
- [26] J.C. Dyre, Master-equation approach to the glass transition, *Phys. Rev. Lett.* 58 (8) (1987) 792.
- [27] J.C. Dyre, Energy master equation: a low-temperature approximation to bässler’s random-walk model, *Phys. Rev. B* 51 (18) (1995) 12276.
- [28] G.G. Naumis, Simple solvable energy-landscape model that shows a thermodynamic phase transition and a glass transition, *Phys. Rev. E* 85 (6) (2012) 061505.
- [29] D.A. Huse, D.S. Fisher, Residual energies after slow cooling of disordered systems, *Phys. Rev. Lett.* 57 (17) (1986) 2203.
- [30] S.A. Langer, J.P. Sethna, E.R. Grannan, Nonequilibrium entropy and entropy distributions, *Phys. Rev. B* 41 (4) (1990) 2261.
- [31] S.A. Langer, A.T. Dorsey, J.P. Sethna, Entropy distribution of a two-level system: An asymptotic analysis, *Phys. Rev. B* 40 (1) (1989) 345.
- [32] S.A. Langer, J.P. Sethna, Entropy of glasses, *Phys. Rev. Lett.* 61 (5) (1988) 570.
- [33] J.J. Brey, A. Prados, Residual properties of a two-level system, *Phys. Rev. B* 43 (10) (1991) 8350.
- [34] A. Prados, J. Brey, B. Sánchez-Rey, A dynamical Monte Carlo algorithm for master equations with time-dependent transition rates, *J. Stat. Phys.* 89 (3–4) (1997) 709–734.
- [35] K. Trachenko, V. Brazhkin, Heat capacity at the glass transition, *Phys. Rev. B* 83 (1) (2011) 014201.
- [36] T.F. Middleton, J. Hernández-Rojas, P.N. Mortenson, D.J. Wales, Crystals of binary Lennard-Jones solids, *Phys. Rev. B* 64 (18) (2001) 184201.
- [37] T.F. Middleton, D.J. Wales, Energy landscapes of some model glass formers, *Phys. Rev. B* 64 (2) (2001) 024205.
- [38] V.K. de Souza, D.J. Wales, Connectivity in the potential energy landscape for binary Lennard-Jones systems, *J. Chem. Phys.* 130 (19) (2009) 194508.